Experimental Thermal and Fluid Science 33 (2009) 1180–1187

Contents lists available at ScienceDirect

Experimental Thermal and Fluid Science

journal homepage: www.elsevier.com/locate/etfs

Design, testing and two-dimensional flow modeling of a multiple-disk fan

Tahsin Engin *, Mustafa Özdemir, Şevki Çeşmeci

Department of Mechanical Engineering, The University of Sakarya, Esentepe Campus, 54187 Sakarya, Turkey

ARTICLE INFO

Article history:
Received 7 May 2009
Received in revised form 27 July 2009
Accepted 27 July 2009

Keywords:
Flow between co-rotating disks
Multiple-disk fan
Tesla turbine
Multiple-disk pump
Tesla pump

ABSTRACT

A multiple-disk Tesla type fan has been designed, tested and analyzed two-dimensionally using the conservation of angular momentum principle. Experimental results showed that such multiple-disk fans exhibited exceptionally low performance characteristics, which could be attributed to the low viscosity, tangential nature of the flow, and large mechanical energy losses at both suction and discharge sections that are comparable to the total input power. By means of theoretical analysis, local and overall shearing stresses on the disk surfaces have been determined based on tangential and radial velocity distributions of the air flow of different volume flow rates at prescribed disk spaces and rotational speeds. Then the total power transmitted by rotating disks to air flow, and the power acquired by the air flow in the gap due to transfer of angular momentum have been obtained by numerically integrating shearing stresses over the disk surfaces. Using the measured shaft and hydraulic powers, these quantities were utilized to evaluate mechanical energy losses associated with the suction and discharge sections of the fan.

1. Introduction

Despite the geometrical simplicity, the study of viscous flow between two rotating parallel disks in a fixed enclosure has received considerable interest over the several past decades since the phenomenon is of scientific interest and much practical importance. Examples include, but not limited to, magnetic disk storage industry, chemical reactors, and turbomachinery. In the early times of its invention by Tesla [17], multiple-disk turbomachinery was regarded as conceptual design due to the fact that their efficiency with ordinary fluids is less than that of traditional bladed flow machines.

A literature survey would show that the subject of multiple-disk turbomachinery and flow between co-rotating parallel disk assembly have taken noticeable interest by several investigators over the past decades. Humphrey et al. [7] studied two- and three-dimensional unsteady laminar flow fields between a pair of disks co-rotating in a fixed enclosure at different Reynolds numbers, and they reported that while three-dimensional calculations were in better agreement with the experimental results than those of two-dimensional analyses, both sets of simulations revealed instability in the region near the curved enclosure wall. As a continuation of this paper, Iglesias and Humphrey [8] observed experimentally that in a critical range of Reynolds number, the flow between two parallel disks evolved from steady axisymmetric to unsteady three-dimensional nature. However, their calculations with an aspect ratio of 0.279 and for $Re > 7715$ resulted in a new, non-unique steady solution for the velocity field that was axisymmetric with respect to inter-disk mid-plane. In a similar fashion, Al-Shannag et al. [1] conducted a numerical analysis in order to investigate the tip clearance effects on the isothermal laminar air flow between co-rotating disks in fixed cylindrical enclosures. They concluded that both two- and three-dimensional analyses using the boundary conditions in the gaps fail matching the experimentally measured radial variations of the mean and *rms* tangential velocity components in the inter-disk space. As a consequence, they suggested using computationally intensive three-dimensional calculations of the entire flow domain encompassing tip clearances (gaps), which yield results that were in fairly good agreement with the measured mean and *rms* velocities. Mazza and Rosa [10] modeled turbulent flow between a pair of co-rotating disks using Reynolds Averaged Navier–Stokes (RANS) equations and a two-equation turbulence model employing isotropic eddy viscosity. They pointed out that the predicted pressure rise increased as the rotational speed elevated. Also, they concluded that the pressure rise in the vicinity of the inlet of the disks was due to divergence in the cross-sectional area of the channel, while further away from the inlet it was found to be proportional to the centrifugal force developed. Miura and Mizushima [13] numerically studied transitions of flow between co-rotating disks in a fixed cylindrical enclosure. In their study, the flow was not only symmetric with respect to inter-disk mid-plane but also axisymmetric about the axis of rotation at low Reynolds numbers, whereas it was unstable at large ones. They examined symmetry-breaking instability with respect to inter-disk mid-plane assuming the flow field to be axisymmetric, and obtained numerically the steady axisymmetric flows. Torok and Gronseth [18] analyzed numerically the

* Corresponding author. Tel./fax: +90 264 346 0555.
E-mail addresses: engint@sakarya.edu.tr, tahsinengin@yahoo.com (T. Engin).

0894-1777/$ - see front matter © 2009 Elsevier Inc. All rights reserved.
doi:10.1016/j.expthermflusci.2009.07.007

Nomenclature

D	disk outer diameter (m)
d	disk gap (m)
D_h	equivalent hydraulic diameter (m)
f	Fanning friction factor (–)
H	angular momentum (kg/m^2 s^2)
j	number of independent variables
$\dot{m}$	mass flow rate (kg/s)
n	number of revolutions (rpm)
N	number of disks (–)
P	pressure (Pa)
Q	volume flow rate (m^3/s)
r	radial coordinate (m)
$u(y)$	uncertainty in the parameter y
x_i	independent variable involved
$u(x_i)$	standard uncertainty of ith independent variable
u_θ	tangential component of the absolute velocity (m/s)
v_r	radial component of the absolute velocity (m/s)
$\dot{W}_{air}$	mechanical power acquired by air (W)
$\dot{W}_{air,fcv}$	mechanical power acquired by air (Eq. (12)) (W)
$\dot{W}_{disk}$	mechanical power transmitted to fluid by disks (W)
$\dot{W}_{hyd}$	hydraulic power (W)
$\dot{W}_{loss}$	lost mechanical power (W)
$\dot{W}_{shaft}$	shaft power (W)
η_d	disk suction efficiency (–)
η_e	overall fan efficiency (–)
η_f	impeller efficiency (–)
η_h	discharge efficiency (–)
ρ	density (kg/m^3)
ω	angular velocity (rad/s)
τ_w	wall shear stress (N/m^2, Pa)
$\tau_{w\theta}$	local wall shear stress (N/m^2, Pa)

flow and thermal fields between co-rotating disks in fixed channels using axisymmetric flow model, and determined velocity and temperature fields via a commercial CFD code. Their numerical simulations showed a rotating core region, which was seen to cover approximately the inner third of the gap. The outer two-thirds of the gap, on the other hand, was observed to be consisted of a recirculation region with fluid in the vicinity of the disk being transported radially outward due to disk rotation, and being drawn radially inward due to momentum exchange. More recently, Soong et al. [16] investigated experimentally the three-dimensional flow field between two co-axial disks rotating independently. They handled the problem in a very systematic manner and discovered distinct flow structures in the gap for different running conditions. Their findings could be regarded to provide profound insights for better understanding the dynamics of flows between co-axially rotating disks that is still involving much complex underlying physics.

A Tesla-type pump or fan is an unconventional centrifugal turbomachinery that uses smooth disks instead of blades. Despite their low-efficiency characteristics, multiple-disk pumps offer several remarkable advantages over the conventional vaned impeller pumps such as having greater stability, low sensitivity to cavitation, ability to handle unusual fluids, e.g., highly viscous fluids, gas–liquid mixtures, highly concentrated commercial slurries and suspensions, and non-Newtonian fluids. Tesla pumps are also very promising in biomedical applications, in which they are generally used to pump the blood as an artificial hearth [11,12]. Although the early studies on the multiple-disk pump primarily date back to 1960s [6,14,2,4] the problem was first handled both experimentally and numerically in a systematic manner by Roddy et al. [15], who confirmed the general affinity laws, by which disk pump performance can be characterized as a function of some groups of parameters representing the dimensional head, power, efficiency, gap space, and Reynolds number, through employing a theoretical analysis relying on the principle of momentum transfer.

Despite of a large number of investigations on the flow structures between two rotating parallel disks and in the multiple-disk pumps, there is no systematic treatment of flow analysis and performance characterization of multiple-disk fans in the open literature. The use of multiple-disk configuration in conventional casings is quite favorable in some processes due to the fact that they offer low friction losses, which is very important for handling viscous fluids. They also suggest simplicity in manufacturing, and are favorable for coating surfaces with some protective materials such as ceramics. These fans are also of particular interest when operated to handle hot gases at elevated temperatures, e.g., exceeding 800 °C. Some industrial processes require hot gases being conveyed at elevated temperatures to increase the product quality, to reduce the energy consumption and gas emissions. Examples may include glass industry, some chemical engineering processes, ceramic industry, and some metallurgical engineering processes. The three-dimensionally optimized steel fan impellers can be safely operated at the temperatures up to 800 °C. On the other hand, the mechanical strength of the steel materials drops drastically due to both high temperatures exceeding 600 °C and increased centrifugal forces acting on the impeller blades [5]. In the case of such high temperature gases, the priority is generally to convey the gas rather than expectation of high performance characteristics, and two-dimensional multiple-disk fans are best fit to those applications.

The present study deals with the experimental and theoretical characterization of a multiple-disk fan operating under atmospheric conditions. The analysis relies on the principle of conservation of angular momentum. The effect of gap width, and rotational speed have been numerically investigated for both design and off-design volume flow rates. In addition, the variations of velocity components, friction factor, local shear stress and total shear stress over the disk surfaces have been obtained, and used to determine fan pressure rise and related efficiencies.

2. Experimental study

Experiments were conducted on a specially designed and fabricated set-up in order to ascertain performance characteristics of the multiple-disk fan under atmospheric conditions. The schematic layout of the set-up is illustrated in Fig. 1. The set-up, which was built in accordance with the DIN24163 standard, consisted of three sections, namely *motor-speed reducer group*, *test fan*, and *measurement line*. The fan was driven with a 1 kW-DC motor whose speed could be flexibly adjusted between 0 and 3000 rpm. The power generated by the motor was determined based on the actual measurements of electric current and voltage. The net power transmitted to the fan shaft at different rotational speeds was determined by taking the difference in powers measured with and without the test fan. The rotational speed was measured by means of an optical tachometer. The measurement line was made with PVC with an inner diameter of 150 mm. The volume flow rate of air

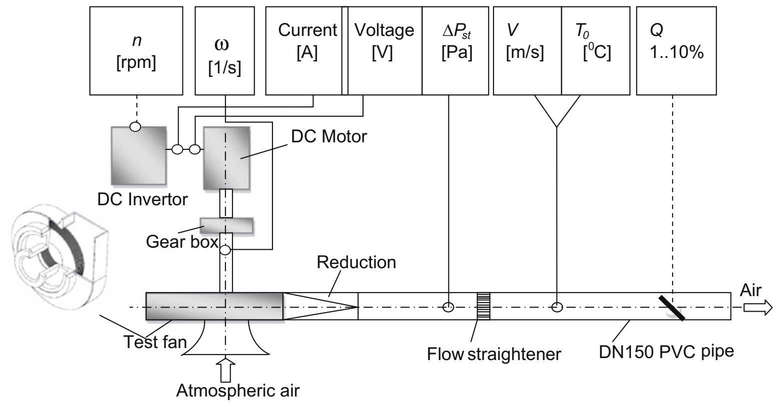

Fig. 1. Schematic layout of the experimental set-up.

was determined based on the velocity measurements made by a hot-wire anemometer installed in the test section. The flow rate was varied by employing a damper provided at the end of test section. The calibration of each meter was checked before and after each test run. All measurements of pressure, temperature, fan speed, flow velocity, and the power transmitted to the motor shaft were made using electronic transducers, and the electrical signals corresponding to these physical quantities were collected by a data acquisition and control system commanded by a PC. Care was also taken to ensure that the flow reached steady-state conditions, and all measurements were made in the hydrodynamically fully-developed flow regions.

The multiple-disk fan was specially designed and fabricated in the Energy Techniques Institute at the Clausthal Technical University, Germany. The meridional profile and side-view of the test fan are schematically shown in Fig. 2. The disk pack impeller was designed in such a way that it consisted of various number of parallel disks. Since the pack width is limited to 50 mm, the number of disks dictates the gap size. Totally 11, 13, and 15 disks were installed in the disk pack corresponding 1 mm, 1.5 mm, and 2 mm of disk spacing, respectively. A separate rear disk was connected to the fan shaft, and the other disks were fixed to each other by using four pins, which were 5 mm in diameters and arrayed such that they had 90° between each other. The inner and outer diameters of each disk, having a thickness of 3 mm, were 125 mm and 275 mm, respectively. The specific speed of the impeller is 350 rpm according to $n_s = 3.65n\sqrt{Q}/H^{3/4}$, where n is the fan speed (rpm), Q is the fan capacity (m^3/s), and $H = \Delta P/\rho g$ fan head (m), ΔP is the fan pressure rise (Pa), ρ is the air density (kg/m^3), g and is the gravitational acceleration (m/s^2), respectively.

3. Two-dimensional modeling of air flow in the gap

A theoretical analysis can be performed for the flow between two co-rotating parallel disks by applying the principle of conservation of angular momentum to a differential fluid particle at a distance of r from the center of rotation, as shown in Fig. 3.

In the $r\theta$-plane:

$$dH = 2dF \cdot r \tag{1}$$

where $H = \dot{m}u_\theta r$ is the angular momentum, $\dot{m}$ is the mass flow rate between two disks, u_θ is the tangential velocity of air flowing in the

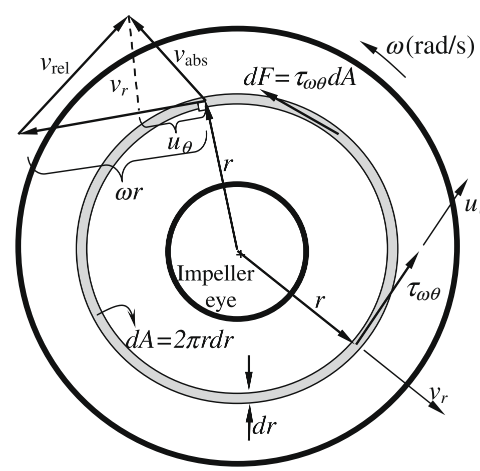

Fig. 3. Differential fluid element, velocity components and exit velocity triangle on a circular disk.

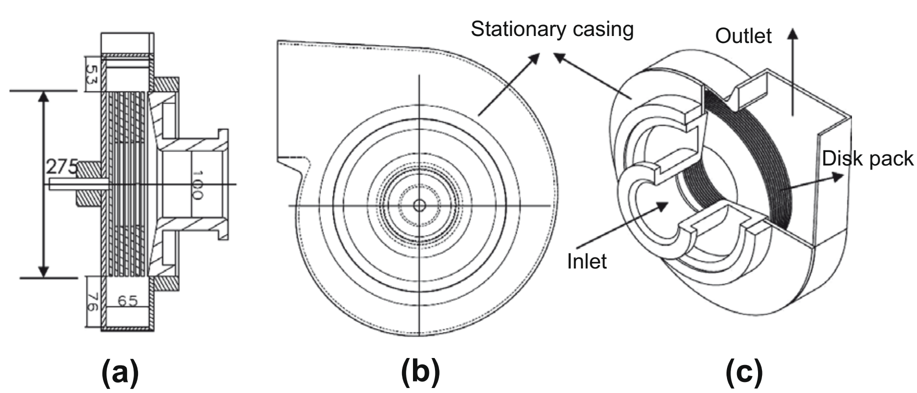

Fig. 2. Schematic of multiple-disk fan: (a) meridional profile, (b) side-view, and (c) three-dimensional view.

gap. Differential shearing force dF due to local wall shear stress $\tau_{w\theta}$ can be expressed by $dF = \tau_{w\theta} dA = \tau_{w\theta} 2\pi r dr = 2\pi\tau_{w\theta} r dr$. The constant 2 in Eq. (1) is put in order to consider two parallel surfaces per gap. Therefore Eq. (1) can be expanded and re-arranged to give

$$\frac{du_\theta}{dr} = \frac{4\pi r \tau_{w\theta}}{\dot{m}} - \frac{u_\theta}{r} \tag{2}$$

The wall shear stress in the disk passage can be given in terms of Fanning friction factor f such that:

$$\tau_w = f\frac{\rho v_{\text{rel}}^2}{2} \tag{3}$$

where ρ is the constant fluid density, since the compressibility effects are negligible. It is clear from Fig. 3 that relative velocity (v_{rel}) can be given in terms of disk peripheral speed (ωr), tangential component of the absolute velocity (u_θ), and radial component of the absolute velocity (v_r) as follows:

$$v_{\text{rel}}^2 = (\omega r - u_\theta)^2 + v_r^2 = (\omega r - u_\theta)^2 + \left(\frac{Q}{(N-1)2\pi r d}\right)^2 \tag{4}$$

where Q is the total volume flow rate, N is the number of rotating disks, and d is the gap width. It should be noted that the mass flow rate through each gap was assumed to be identical. By substituting Eq. (4) into Eq. (3), the total shear stress on the disks can be written as

$$\tau_w = f\frac{\rho}{2}\left[(\omega r - u_\theta)^2 + \left(\frac{Q}{(N-1)2\pi r d}\right)^2\right] \tag{5}$$

In order to make Eq. (2) solvable, the local wall shear stress must be expressed in terms of u_θ as done for τ_w in Eq. (5). The Fanning friction factor can be regarded (or assumed) as an isotropic quantity in the gap, e.g., it is constant in all directions at a particular radial location. Hence, by realizing from Eq. (3) that the wall shear stress is proportional to the square of relative velocity, an approximate relation between τ_w and $\tau_{w\theta}$ can be constructed as follows:

$$\frac{\tau_{w\theta}}{\tau_w} = \frac{(\omega r - u_\theta)^2}{v_{\text{rel}}} \tag{6}$$

since $\tau_w \sim v_{\text{rel}}^2$ and $\tau_{w\theta} \sim (\omega r - u_\theta)^2$. By combining Eqs. (3) and (6), we obtain

$$\tau_{w\theta} = f\frac{\rho}{2}(\omega r - u_\theta)^2 \tag{7}$$

Finally, substitution Eq. (8) into Eq. (2) yields the following first-order non-linear ordinary differential equation for u_θ:

$$\frac{du_\theta}{dr} = \frac{2\pi(N-1)fr}{Q}(\omega r - u_\theta)^2 - \frac{u_\theta}{r} \tag{8}$$

since $\dot{m} = \rho Q/(N-1)$. There is no closed form of solution for Eq. (8), hence it has to be solved numerically. Although Moody diagram could be used to determine Fanning friction factor, from a computer-aided-calculation point of view, it should be in a mathematical relation form. Depending on the radial position on the disk, the flow could be either laminar or turbulent, and the Churchill equation, which is valid for both flow regimes, can be used to estimate Fanning friction factor

$$f = 2\left[\left(\frac{8}{Re}\right)^{12} + \left(\frac{1}{A+B}\right)^{\frac{3}{2}}\right]^{\frac{1}{12}} \tag{9}$$

where $Re = D_h v_{\text{rel}}/v$, D_h is the equivalent hydraulic diameter, v is the kinematic viscosity of air, A and B are the parameters depending on Re number and equivalent hydraulic diameter [3]. Hydraulic diameter has been taken to be $D_h = 2d$ based on infinite parallel plate approximation.

Once tangential velocity component u_θ is determined, the useful power transmitted to the air flow by the disk pack can be evaluated. In order to determine the total power transmitted by disks to the air flowing in the gap, one can integrate differential shearing force dF_θ acting on the fluid element:

$$d\dot{W}_{disk} = dF_\theta \cdot (\omega r) = \tau_{w\theta} dA \cdot (\omega r) \text{ or}$$
$$\dot{W}_{disk} = 2N\omega \int_{r_1}^{r_2} \tau_{w\theta} r dA \tag{10}$$

The power acquired by air can then be expressed in a similar fashion

$$\dot{W}_{air} = 2N\int_{r_1}^{r_2} \tau_{w\theta} dA \tag{11}$$

The difference between these two powers will give the power loss due to friction, that is $\dot{W}_{loss} = \dot{W}_{disk} - \dot{W}_{air}$. With the measured shaft power $\dot{W}_{shaft}$, various efficiencies can be defined and used to evaluate the overall performance of the test fan:

Loss type	Efficiency
Bearings and disk suction	$\eta_d = \frac{\dot{W}_{disk}}{\dot{W}_{shaft}}$
Disk friction	$\eta_f = \frac{\dot{W}_{air}}{\dot{W}_{disk}}$
Casing and discharge	$\eta_h = \frac{\dot{W}_{hyd}}{\dot{W}_{air}} = \frac{\Delta PQ}{\dot{W}_{air}}$
Overall fan efficiency	$\eta_e = \eta_d\eta_f\eta_h = \frac{\Delta PQ}{\dot{W}_{shaft}}$

Here η_d, η_f, and η_h represent the mechanical energy losses associated with the journal bearings and impeller entry, friction in the disk gaps, and casing and discharge losses, respectively.

In addition, the results obtained from numerical analysis have been non-dimensionalized by the following definitions:

$$d^* = \frac{d}{D} \quad \Delta P^* = \frac{\Delta P}{\rho\omega^2 D^2}$$
$$Q^* = \frac{Q}{\omega D^3} \quad \dot{W}^* = \frac{\dot{W}}{\rho\omega^3 D^5}$$

4. Results and discussions

Experiments were performed with 11, 13, and 15 disks in the fan, yielding a gap width of 1 mm, 1.5 mm, and 2 mm, respectively. Volume fraction of disks in the fan casing was kept the same for different gap widths, so that a much more reasonable comparison of different disk numbers within the single pack could be made. Tests were done at 1500, 2000, 2500, and 3000 rpm. Using accepted error analysis, the combined uncertainty associated with a dependent parameter as a function of other measured independent variables, $y = f(x_1, x_2, \ldots, x_n)$ can be expressed as

$$u(y) = \sqrt{\sum_{i=1}^{j}\left(\frac{\partial f}{\partial x_i}u(x_i)\right)^2} \tag{12}$$

where $u(y)$ is the uncertainty in the parameter y, x_i's are the variables of functional dependence, and $u(x_i)$ is the standard uncertainty in the measurement of each functionally dependent variable x_i [9]. The standard uncertainty of each measured quantity has been estimated based on the resolution of each corresponding meter, by assuming a rectangular distribution (Table 1). Since there is no uncertainty statement accompanying the density and dynamic viscosity of air, they are assumed to be known to within their last significant digits.

Table 1
Uncertainty estimates of measured and derived parameters.

Measured quantity	Standard uncertainty
Fan speed (N)	±0.6 rpm
Motor voltage (V)	±0.5 mV
Motor current (A)	±0.05 mA
Hot-wire anemometer (V)	±0.03 m/s
Pressure difference (ΔP)	±0.05 Pa
Temperature (T = 20 °C)	±0.1 °C
Air density (tabulated data: ρ = 1.204 kg/m^3)	$\pm 2.3 \times 10^{-3}$ kg/m^3
Air viscosity (tabulated data: $\mu = 1.825 \times 10^{-5}$ Pa s)	$\pm 3 \times 10^{-8}$ Pa s
Derived non-dimensional quantity	
Q^*	$\pm 9 \times 10^{-4}$
ΔP^*	$\pm 4 \times 10^{-5}$
$\dot{W}^*_{hyd}$	$\pm 2 \times 10^{-5}$
$\dot{W}^*_{shaft}$	$\pm 2 \times 10^{-5}$
η_e	$\pm 5 \times 10^{-9}$
d^*	$\pm 7 \times 10^{-5}$
Re	±1

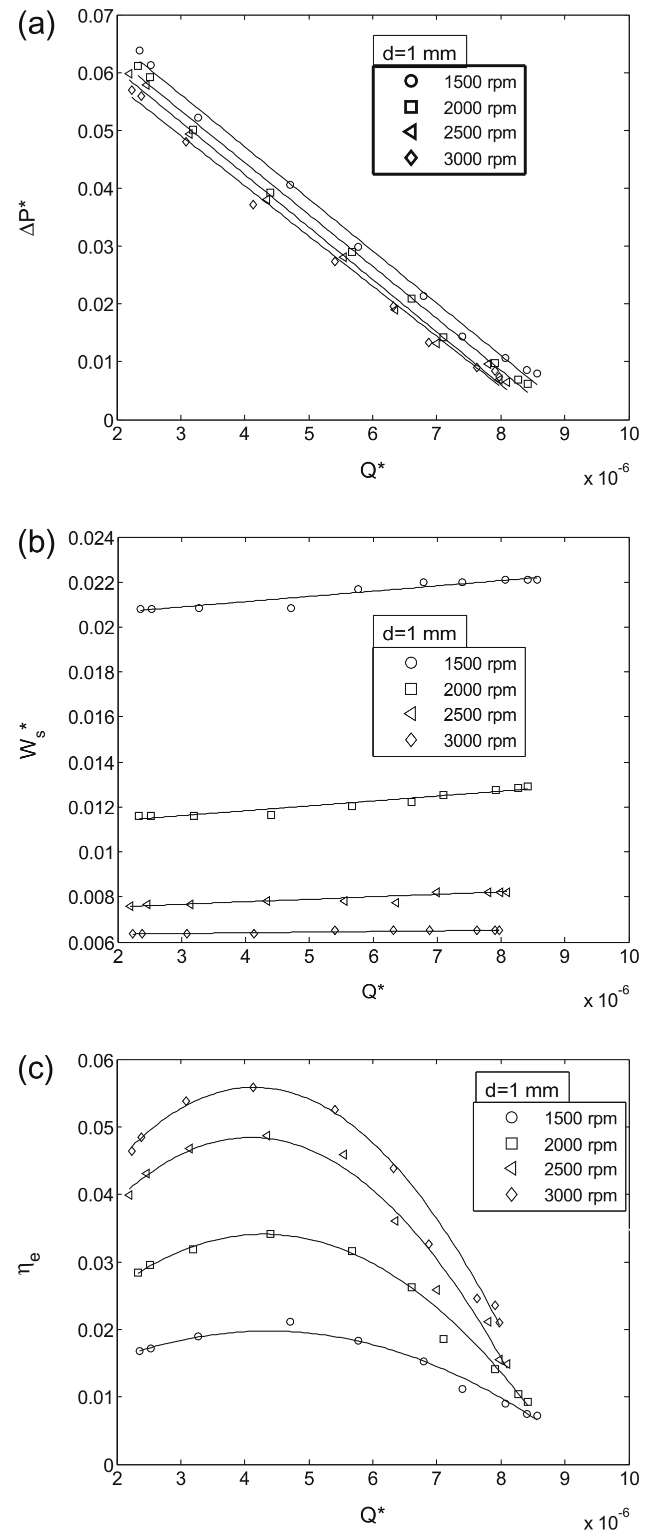

Fig. 4. Non-dimensional performance characteristics of the fan for $d = 1$ mm ($d^* = 3.63 \times 10^{-3}$) disk gap at different rotational speeds: (a) pressure rise vs. flow rate, (b) shaft power vs. flow rate, and (c) overall efficiency vs. flow rate.

4.1. Experimental results

Non-dimensional performance characteristics of the test fan with 15 disks at four different rotational speeds are shown in Fig. 4a–c. It is clearly seen from Fig 4a that the pressure rise varies linearly with the volume flow rate. At a particular flow rate, however, it is interesting to observe higher pressure rises for the higher rotational speeds. Since this is a non-dimensional representation, one may expect that all straight lines of different speeds coincide with each other, and look like a single line. This is the case if the similarity laws for turbomachinery were to hold for this Tesla-type unconventional rotary fan. Hence we conclude that the non-dimensional pressure rise is not only a function of non-dimensional flow rate but also a function of Reynolds number based on outer peripheral speed of the disk impeller ($Re_D = \omega D^2/\upsilon$). As for non-dimensional shaft power, Fig. 4b shows that the input power to the fan increases slightly as the flow rate increases; however, these orders of increase in the shaft power can be disregarded for practical applications. There is, however, a clear dependence on Reynolds number as the non-dimensional pressure rise. Although such a dependence on Reynolds number is not seen for conventional vaned turbomachinery, this is the case that may be encountered in multiple-disk flow machines. A pretty similar observation was also reported by Roddy et al. [15] for a commercial large-scale centrifugal multiple-disk pump. The overall fan efficiency η_e vs. non-dimensional flow rate is also shown in Fig. 4c. The peak efficiency increases as the rotational speed increases ranging from 2% at 1500 rpm to around 6% at 3000 rpm! It is well-known that the Tesla-type centrifugal pumps exhibit generally low performance characteristics, and the results showed that the multiple-disk fans are much more inefficient flow machines as compared to the same kind of pumps. This is primarily due to very low viscosity of air and unavoidable mechanical energy losses experienced throughout the fan as discussed in the following subsections in more detail. It is also evident from Fig. 4c that the overall fan efficiency depends on more than just non-dimensional volume flow rate, since all of the data points do not fall on a single curve as declared by the similarity laws. This is not surprising since both pressure rise and shaft power are also dependent on fan Reynolds number. Very similar trends have been recorded for the other number of disks, that is, for 13 and 11 disks corresponding to a disk gap of 1.5 mm, and 2 mm, respectively.

4.2. Numerical results and discussions

The structure of the flow field between two rotating disks depends largely on flow regime. Therefore, it would be interesting to see what happens in the gaps of the disk pack, since the Reynolds numbers experienced at the test speeds indicate both laminar and turbulent flow regimes. The air velocity relative to the rotating disk surface decreases from inlet to outlet due to divergence in the cross-sectional area at a given volume flow rate,

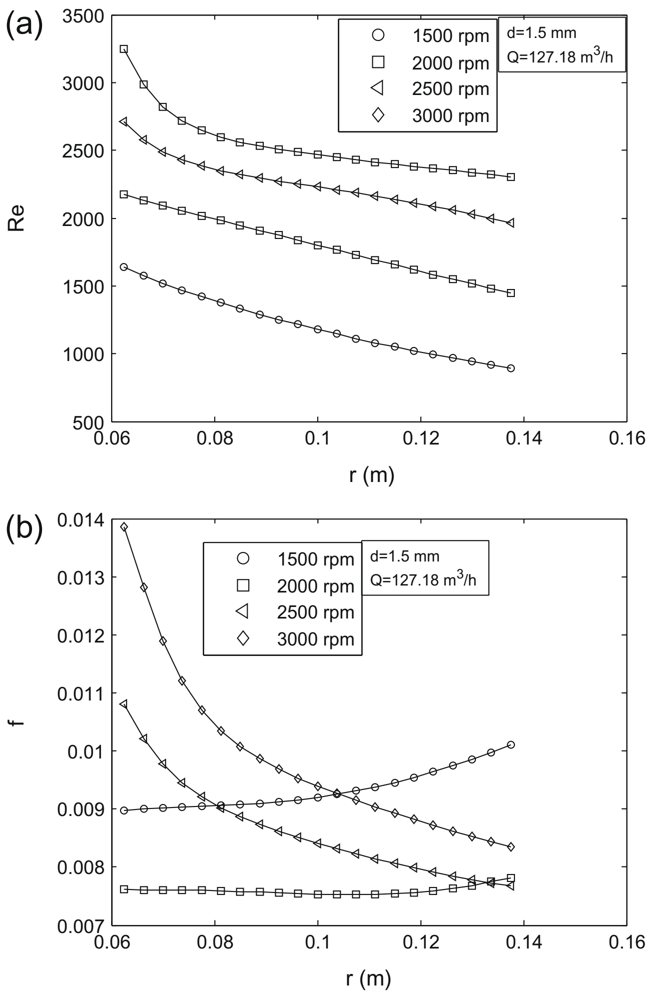

Fig. 5. (a) The variation of *Re* number with the radial coordinate in the gap for 127.18 m^3/h ($Q^*_{@1500\ \mathrm{rpm}} = 0.011$) and *d* = 1.5 mm ($d^*$ = 5.45 × 10^{-3}). (b) The variation of Fanning friction factor within the gap for 127.18 m^3/h and *d* = 1.5 mm.

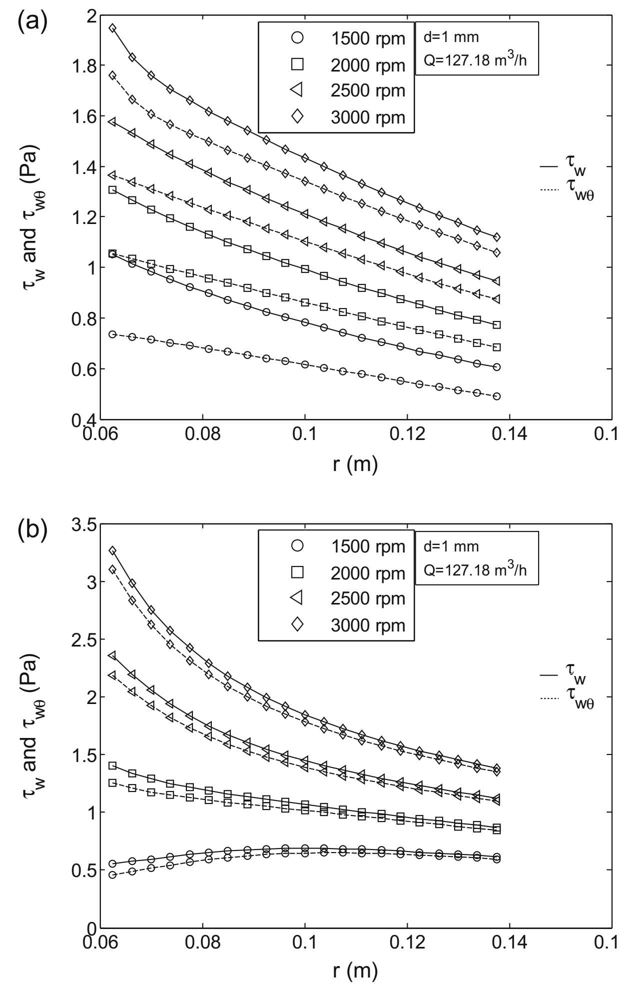

Fig. 6. The variation of total and local shear stresses with the radial coordinate in the gap at 127.18 m^3/h ($Q^*_{@1500\ \mathrm{rpm}} = 0.011$): (a) for disk gap *d* = 1 mm (d^* = 3.63 × 10^{-3}) and (b) for disk gap *d* = 2 mm (d^* = 7.26 × 10^{-3}).

tending the Reynolds number $Re = D_h v_{\mathrm{rel}}/\nu$ to decrease. For *d* = 1.5 mm (d^* = 5.45 × 10^{-3}), and at a fixed flow rate of 127.18 m^3/h ($Q^*_{@1500\ \mathrm{rpm}} = 0.011$), the flow between disks is laminar for 1500 and 2000 rpm, and is turbulent for 2500 and 3000 rpm, as shown in Fig. 5a. Due to this reason, the Fanning friction factor exhibits very distinct variation within the range of radial coordinate *r* (Fig. 5b).

A similar distinction is also observed for total wall shear stress and local shear stress, the later is directly related to power acquired by the rotating disks. The variation of both shear stresses vs. radial coordinate at the same flow rate is shown non-dimensionally in Fig. 6a and b for *d* = 1 mm, and 2 mm, respectively. It is evident from Fig. 6a that both shear stresses decrease as *r* increases for *d* = 1 mm, and the difference between these two stresses remain nearly the same in the disk passage. This is what happens in the laminar flow between disks. Furthermore, it should be noted that there is a noticeable difference between these two stresses due to narrower gap size. As for the turbulent flow seen at the same flow rate when disk gap is enlarged to 1.5 mm or higher (i.e., 2 mm), both curves get closer to each other, that is tangential shear stress component dominates the total wall shearing stress, and radial component of the wall shear stress loses its effect as the gap height increases. This is essentially not surprising since the flow becomes more tangential with the increase in the gap size. Tangential nature of the flow in the multiple-disk turbomachinery is primarily responsible for the low performance characteristics of such machines, since tangential flow in the gaps of the disk pack produces relatively low component of absolute velocity generating moment-of-momentum, i.e., angular momentum.

The mechanical energy acquired by air as a result of rotating disk pack can also be evaluated by choosing an angular region that encloses the impeller section as a control volume. Realizing that only the tangential velocity components contribute to torque, the application of the angular momentum equation to this control volume gives rise to

$$\dot{W}_{air,fcv} = \rho Q \omega (r_2 u_{\theta,2} - r_1 u_{\theta,1}) \tag{13}$$

where subscript denotes *fcv* "finite control volume". Eq. (13) may be regarded as a check on the values of a $\dot{W}_{disk}$ and $\dot{W}_{air}$ calculated numerically from Eqs. (10) and (11), respectively. A quantitative comparison among $\dot{W}_{disk}, \dot{W}_{air}$, and $\dot{W}_{air,fcv}$ is illustrated in Fig. 7, which was constructed for three different gap sizes and four different rotational speeds. It is clear from Fig. 7 that there is an excellent agreement between $\dot{W}_{disk}$ and $\dot{W}_{air,fcv}$, revealing the internal consistency of the numerical calculations. The maximum deviation from the ideal line was observed to be less than 8%.

In order to evaluate overall performance of the multiple-disk fan, various efficiencies defined earlier have been computed and plotted for different rotational speeds and gap sizes as shown in Fig. 8a and b. Fig. 8a shows that, for a disk spacing of 1 mm, impeller efficiency (η_f) varies from about 40% to 80%, and decreases as

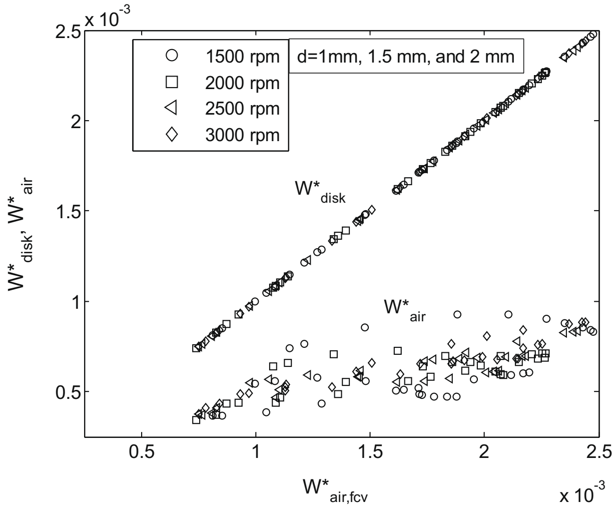

Fig. 7. Comparison of various non-dimensionalized powers associated with the test fan for different gap sizes and rotational speeds.

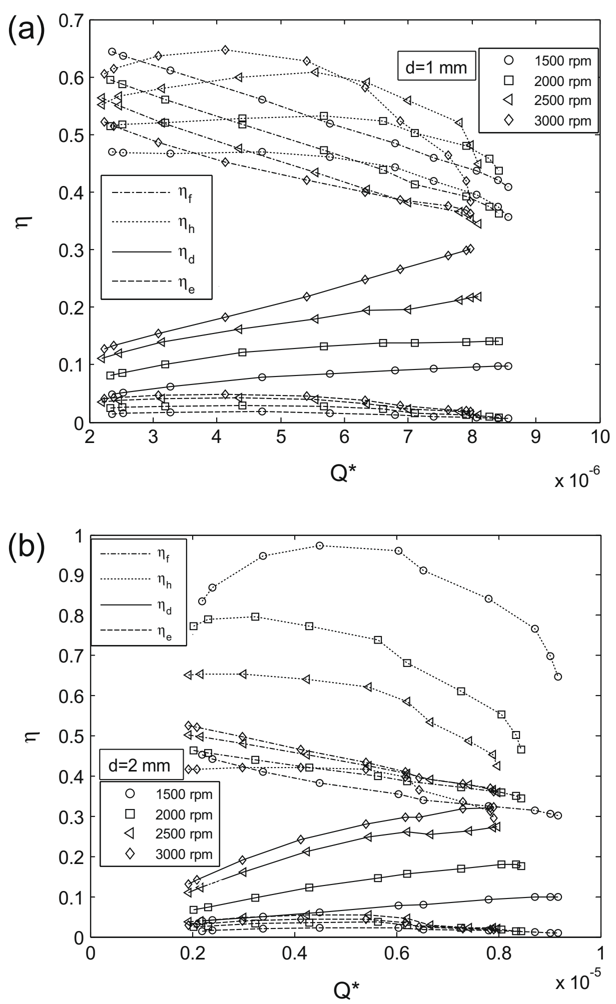

Fig. 8. Comparison of various efficiencies associated with the test fan for different gap sizes and rotational speeds.

the flow rate increases. This is, as expected, due to increase in the frictional loss, which is proportional to square of relative velocity of air in the gap. Disk suction efficiency (η_d), on the other hand, ranges from about 5% to 30% depending on volume flow rate and rotational speed. As opposed to impeller efficiency, disk suction efficiency increases as the flow rate increases. This is primarily due to the fact that the bearing friction would become comparable with the useful power transmitted to the impeller at the lower flow rates, and become less important at the higher flow rates. Probably the most striking result, however, is that the level of disk suction efficiency is seen as exceptionally low compared to conventional vaned blowers, even to multiple-disk pumps. Roddy et al. [15], for instance, reported disk suction efficiencies ranged from 30% to 95% for a large commercially available multiple-disk pump. This also explains why a multiple-disk fan exhibits very low performance characteristics. The majority of the power delivered by the fan shaft is lost in the mechanical bearings. Casing or discharge efficiency (η_h), on the other side, was observed to vary from about 40% to 65%. This is smaller a little bit as compared with the typical values of 60–70% for conventional vaned pumps. This is mostly due to the tangential nature of flow in the disk fans. Similar conclusions were also drawn by Roddy et al. [15] for the multiple-disk pump they tested. As the overall fan efficiency (η_e) is the multiplication of η_d, η_f and η_h, we have to expect dramatically low fan efficiency, as shown in Fig. 8a and b. The variation of the overall efficiency was seen to be squeezed in a narrow band ranging from about 2% to 6%!. Although the efficiencies at such low levels for conventional turbomachinery could not be regarded as reasonable from an economical point of view, there are several processes requiring industrial gas circulation at very elevated temperatures (above 900 °C), where conventionally vaned fans or blowers with steel impeller could not be operated. Therefore for such exceptional processes, the fulfilling of the process comes first and efficiency of the fan is of no interest.

Very similar tendencies were also observed for other disk gaps as shown in Fig. 8b, where disk gap was $d = 2$ mm. η_f varies from about 30% to 53%, η_d varies from about 4% to 32%, η_h varies from about 30% to 97%, and finally the total efficiency η_e varies from about 1% to 5%. As compared to $d = 1$ mm, disk suction efficiency (η_d) seems to be unchanged. This is expected since η_d is primarily related to the bearing and suction sections. The impeller efficiency, η_f, on the other hand, was found to decrease considerably. This is presumably due to reduced viscous effects affecting angular momentum transfer between rotating disk pack and air flow. Since this type of impellers work based on viscous shearing, enlargement of gap size usually results in reduced impeller efficiency. Due to reduced suction and impeller efficiencies, the overall efficiency was also seen to noticeably decrease.

All of four efficiencies are also seen to have a remarkable dependency on rotational speed of the fan. This is not surprising since both pressure rise and shaft power were found to be strongly affected by the rotational speed. As can be seen from Fig. 8, although the disk suction and casing-discharge efficiencies are strongly affected by the shaft speed, impeller efficiency and consequently overall efficiency exhibit much less sensitivity to the rotational speed.

5. Conclusions

Having performed a comprehensive literature review about the flow dynamics between two rotating disks, the performance characteristics of a multiple-disk centrifugal fan were studied both experimentally and theoretically. Experimental results showed that such multiple-disk fans exhibited exceptionally low performance characteristics, which could be attributed to the low viscosity, tangential nature of the flow, and large mechanical energy losses at both suction and discharge sections, which are comparable to the total input power.

The test results also revealed that the flow regime between the rotating disks could be both laminar and turbulent depending on Reynolds number, which also varies with the radial coordinate measured from the axis of rotation. It was observed that gap spacing plays a major role on the development of the flow between disks. As the gap width is enlarged, the magnitudes of total wall shear stress and its tangential component are of nearly the same order revealing that the tangential shear stress component dominates the total wall shearing stress, and the effect of radial component of the wall shear stress loses its effect as the gap increases. Therefore, it can be concluded that the tangential nature of the flow in the multiple-disk turbomachinery is primarily responsible for the low performance characteristics of such machines, since tangential flow in the gaps of the disk pack produces relatively low component of absolute velocity generating moment-of-momentum, i.e., angular momentum.

In addition to examination of the flow behavior in the gap, the theoretical analysis, which was based on the extension of the transfer of angular momentum principle over a rotating disk, enabled also individual calculation of the total power transmitted from disk pack to air flow, the power acquired by the air flow, and the frictional loss in the gap. With the measured shaft and hydraulic powers, these quantities were then utilized to evaluate mechanical energy losses associated with the suction and discharge sections of the fan. The peak efficiency increases as the rotational speed increases ranging from 2% at 1500 rpm to around 6% at 3000 rpm. Since both pressure rise and shaft power were observed to be dependent on the rotational speed, the overall efficiency was also seen to vary with the shaft speed. Although the efficiencies at such low levels for conventional turbomachinery could not be regarded as reasonable from an economical point of view, there are several processes requiring industrial gas circulation at very elevated temperatures (above 900 °C), where conventionally vaned fans or blowers with steel impeller could not be operated. Therefore for such exceptional processes, fulfillment of the process would come first and efficiency of the fan would be of no interest. In addition, the energy consumption of such multiple-disk fans is often negligible compared to energy intensity of the process. Another important factor on the low efficiency is the fluid (here, air) viscosity. Since this kind of impeller packs are particularly best suited for highly viscous fluids rather than air, the low performance characteristics would be considered as normal. Fortunately, the multiple-disk fans are often designed for aggressive hot gases, and the viscosity of most gases increases as the temperature is elevated. For instance, the dynamic viscosity of the air would almost triple when its temperature is increased from 15 °C to 1000 °C. This would also increase the overall efficiency of the multiple-disk fan.

References

[1] M. Al-Shannag, J. Herrero, J.A.C. Humphrey, F. Girald, Effect of radial clearance on the flow between co-rotating disks in fixed cylindrical enclosures, Journal of Fluids Engineering 124 (2002) 719–727.
[2] O. Balje, A Study on the Performance Potential of Conventional and Shear Force Pumps, ARL Report No. 65-118, 1965.
[3] S. Churchill, Friction factor equation spans all fluid flow regimes, Chemical Engineering (1977) 91–92.
[4] M. Crawford, A Composite Solution Method for Analytical Design and Optimization Studies of a Multiple Disk Pump, M.S. Thesis, Arizona State University, 1972.
[5] T. Engin, M. Gur, R. Scholz, Effects of tip clearance and impeller geometry on the performance of semi-open ceramic centrifugal fan impellers at elevated temperatures, Experimental Thermal Fluid Science 30 (2006) 565–577.
[6] S. Hasinger, L. Kehrt, Investigation of a shear force pump, ASME Journal of Engineering for Power 85 (1963) 201–207.
[7] J.A.C. Humphrey, C.A. Schuler, D.R. Webster, Unsteady laminar flow between a pair of disks co-rotating in a fixed cylindrical enclosure, Physics of Fluids 7 (6) (1995) 1225–1240.
[8] I. Iglesias, J.A.C. Humphrey, Two- and three-dimensional laminar flows between disks co-rotating in a fixed cylindrical enclosure, International Journal for Numerical Methods in Fluids 26 (1998) 581–603.
[9] ISO, Guide to the Expression of Uncertainty in Measurement, International Organization for Standardization (ISO), Geneva, Switzerland, 1995.
[10] R.A. Mazza, E.S. Rosa, Co-rotating disk assembly with turbulent through flow, Numerical Heat Transfer: Part A 53 (2008) 157–177.
[11] G.E. Miller, R. Fink, Analysis of optimal design configurations for multiple disk centrifugal blood pump, Artificial Organs 23 (6) (1999) 559–565.
[12] G.E. Miller, B.D. Etter, J.M. Dorsi, A multiple disk pump as a blood flow device, IEEE Transactions on Biomedical Engineering 37 (2) (1990) 157–163.
[13] T. Miura, J. Mizushima, Transitions of axisymmetric flow between two co-rotating disks in an enclosure, Fluid Dynamics Research 39 (2007) 193–208.
[14] W. Rice, An analytical and experimental investigation of multiple disk pumps and compressors, ASME Journal of Engineering for Power 85 (1963) 191–200.
[15] P.J. Roddy, R. Darby, G.L. Morrison, P.E. Jenkins, Performance characteristics of a multiple-disk centrifugal pump, ASME Journal of Fluids Engineering 109 (1987) 51–57.
[16] C.Y. Soong, C.C. Wu, T.P. Liu, T.P. Liu, Flow structure between two co-axial disks rotating independently, Experimental Thermal Fluid Science 27 (2003) 295–311.
[17] N. Tesla, Turbine, U.S. Patent No. 1061206, 1913.
[18] D.F. Torok, R. Gronseth, Flow and thermal fields in channels between corotating disks, IEEE Transactions on Components, Hybrids, and Manufacturing Technology 14 (4) (1988) 585–593.